

See discussions, stats, and author profiles for this publication at: <https://www.researchgate.net/publication/11585910>

# Involvement of Protein Kinase A in the Phosphorylation of Spermatidal Protein TP2 and Its Effect on DNA Condensation †

ARTICLE *in* BIOCHEMISTRY · FEBRUARY 2002

Impact Factor: 3.02 · DOI: 10.1021/bi0117652 · Source: PubMed

---

CITATIONS

30

---

READS

22

4 AUTHORS, INCLUDING:



[Amom Ruhikanta Meetei](#)

Cincinnati Children's Hospital Medical Center

38 PUBLICATIONS 2,339 CITATIONS

SEE PROFILE



[Ullas Kolthur-Seetharam](#)

Tata Institute of Fundamental Research

25 PUBLICATIONS 596 CITATIONS

SEE PROFILE

# Involvement of Protein Kinase A in the Phosphorylation of Spermatidal Protein TP2 and Its Effect on DNA Condensation<sup>†</sup>

Amom Ruhikanta Meetei,<sup>‡</sup> Kolathur S. Ullas,<sup>‡</sup> V. Vasupradha, and Manchanahalli R. Satyanarayana Rao\*

*Department of Biochemistry, Indian Institute of Science, Bangalore 560 012, India*

*Received September 6, 2001; Revised Manuscript Received October 29, 2001*

**ABSTRACT:** Rat spermatidal protein TP2 is rich in serine residues and has several potential sites for phosphorylation by different protein kinases. Recombinant TP2 is phosphorylated upon incubation in vitro with salt extract of testicular sonication resistant nuclei (SRN) (representing elongating and elongated spermatids). The major phosphorylation sites were localized to the C-terminal, V8 protease-derived, fragment (residues 87–114). Phosphorylation experiments with the wild type and different site-specific mutants of TP2 revealed that serine 109 and threonine 101 are the phosphorylation sites. Phosphorylation of the C-terminal fragment of TP2 was also demonstrated in vivo. Phosphorylation was not stimulated by either protein kinase C activators or cGMP but was inhibited by protein kinase A inhibitor (PKI) peptide, showing the involvement of protein kinase A in the phosphorylation of TP2. Phosphorylation of TP2 greatly reduced its DNA condensation property. TP2 when complexed with DNA was not a good substrate for phosphorylation by PKA. Dephosphorylation of the DNA–TP2 complex by calf intestinal alkaline phosphatase restored the DNA condensation property to a level equivalent to that observed with TP2. The physiological significance of the phosphorylation–dephosphorylation cycle is discussed with reference to the two-domain model of TP2.

Spermiogenesis in mammals is a unique model for cellular differentiation in which the haploid round spermatids mature to highly condensed and transcriptionally inert spermatozoa. This process takes place over 16 days in rat, during which time there is an extensive restructuring of chromatin architecture, shedding of cytoplasm, and formation of the flagellar tail. The changes that occur at the nuclear architectural level bring about transformation of the nucleosomal type of chromatin organization into a smooth nucleoprotamine fiber that is present in the mature epididymal spermatozoa. Mammals, in particular, are rather unique in that they have evolved a transient phase which occurs during stages 12–15 of spermiogenesis wherein the nucleosomal histones are replaced temporarily by a group of basic proteins (TP1, TP2,<sup>1</sup> and TP4) which are themselves replaced finally by protamines during stages 16–19 (1, 2). The transition protein genes are transcribed during stages 10–12, and their mRNAs are stored in the cytoplasm. It is believed that their translation regulation may be achieved by a similar mechanism as has been demonstrated with protamines (3). The in vivo sequence of events that take place during this transition phase has not been amenable for experimentation particularly since (a) there

is no in vitro model for differentiation of round spermatids, (b) the spermatogenesis in mammals is highly asynchronous in nature, and (c) the population of cells undergoing the transition event represent only a very small percentage of the total germ cells that are present in the adult testis. It has been difficult, however, to explain why mammals have evolved this mechanism of maturation of spermatozoa, although in many species there is a direct replacement by protamines. Our work on TP1 and TP2, studying their in vitro DNA binding properties, has shown that while TP1 is a DNA melting protein (4), TP2 is a zinc metalloprotein (5) that recognizes CpG islands preferentially and condenses DNA in a zinc-dependent manner (6–9). We have recently identified two novel zinc finger domains present in TP2 and have further shown that TP2 has a nucleolar localization signal that targets the protein preferentially to the nucleolus in transient transfection experiments using COS-7 cells (10). TP4 has also been shown to induce local destabilization of DNA (11); however, a detailed study of this protein is still awaited.

Protein phosphorylation plays an important role in several intracellular processes, including modulation of function of DNA binding proteins that include histones and transcription factors (12–14). Earlier investigations have shown that protamines are phosphorylated in their basic domains immediately after their synthesis both in trout (15) and in mammals (16–18). After their deposition onto chromatin, protamines become dephosphorylated to allow the basic amino acid residues to interact with the DNA–phosphate backbone to facilitate chromatin condensation. This phosphorylation–dephosphorylation cycle is thought to be necessary for obtaining correct nucleoprotamine positioning during

<sup>†</sup> This work was supported by India's Department of Biotechnology (New Delhi, India).

\* To whom correspondence should be addressed: Department of Biochemistry, Indian Institute of Science, Bangalore 560 012, India. Fax: 91-80-3600814 or 91-80-3600118. E-mail: mrsrao@biochem.iisc.ernet.in.

<sup>‡</sup> These authors contributed equally to this work.

<sup>1</sup> Abbreviations: TP2, transition protein 2; PTP2, phosphorylated TP2; PKA, protein kinase A; PKI, protein kinase A inhibitor peptide; SRN, sonication resistant nuclei; PMSF, phenylmethanesulfonyl fluoride; GST, glutathione S-transferase.

the formation of the nucleoprotamine fiber in the sperm nucleus (19–22). There have been two studies on the phosphorylation status of transition proteins TP1 and TP2. Green et al. (21) showed that TP2 but not TP1 becomes phosphorylated in vivo in both rat and mouse testis immediately after their synthesis. However, they did not characterize the phosphorylation sites or the kinase involved in TP2 phosphorylation. They predicted that serine-proline dipeptide units present in TP2 might be the sites of phosphorylation. In a recent report, Levesque et al. (23) showed that recombinant TP1 and TP2 can be phosphorylated in vitro by purified kinases, A and C. They further showed that phosphorylation by protein kinase C affected the DNA condensing ability of TP2 as measured with the protein-mediated ligation assay. However, they have also not identified the phosphorylation sites that can be phosphorylated in vitro. Here we report a detailed analysis of phosphorylation of TP2 by using salt extract of sonication resistant nuclei. With a series of experiments involving inhibitors and mutants of TP2, we show that protein kinase A is the predominant kinase involved in the phosphorylation of serine 109 and threonine 101. The major sites of in vivo phosphorylation of TP2 were also found to be localized at the C-terminal third of the TP2 module as observed with SRN extract in vitro. We have also observed that this phosphorylation strongly inhibits the DNA condensing property of TP2, which could be relieved by treating the DNA-PTP2 complex with calf intestinal phosphatase.

## EXPERIMENTAL PROCEDURES

*Isolation of Sonication Resistant Nuclei and Preparation of Salt Soluble Extract.* Sonication resistant nuclei were prepared from rat testes according to the method described by Platz et al. (24) with minor modifications. All operations were carried out at 4 °C or on ice. Approximately 50 g of decapsulated rat testes from 60-day-old Wistar rats were homogenized in 6 volumes of buffer A [10 mM Tris-HCl (pH 7.5), 0.1 mM PMSF, 0.34 M sucrose, and 0.1% Triton X-100]. The homogenate was filtered through two layers of cheesecloth and centrifuged at 500g for 10 min. The pellet of crude nuclei was suspended in 3–5 volumes of buffer B [10 mM Tris-HCl (pH 7.4) and 0.1 mM PMSF] and subjected to sonication using a Branson model B-30 sonifier. The sonicate was centrifuged at 8000g for 10 min, and the resulting pellet contained both elongating and elongated spermatid nuclei. The pellet was resuspended in 3–5 volumes of buffer B, and the suspension was layered over a 10 mL cushion of 1.5 M sucrose in buffer B. After centrifugation at 8000g for 30 min, the pellet contained sonication resistant nuclei that were >98% pure.

The salt soluble extract of SRN was prepared with a buffer containing 20 mM Tris-HCl (pH 7.5), 200 mM NaCl, 1 mM benzamidine, 0.2 mM PMSF, 4 mM EDTA, and 0.04% Nonidet P40. The protein concentration was adjusted to approximately 1 µg/µL with the same buffer.

*Generation of TP2 Mutants and Purification of Recombinant Proteins from Escherichia coli.* The cloning of TP2 cDNA, generation of partial synthetic cDNA, and optimization of its expression in *E. coli* were reported recently (25, 26). All the mutants of TP2 carrying single and multiple

mutations were generated in a single PCR product as described previously (27). The desired mutations were confirmed by DNA sequencing in an ABI 377 automated DNA sequencer using dye-terminator chemistry. The wild type and TP2 mutants were purified from IPTG-induced BL21(DE3) cells, in a single step using a heparin–agarose column. Briefly, the cells were lysed in a buffer containing 50 mM Tris-HCl (pH 8.0), 0.57 M NaCl, 10 mM β-mercaptoethanol, and 0.2 mM PMSF. The supernatant collected after centrifugation at 100000g for 1 h was loaded onto the heparin–agarose column, which was pre-equilibrated with the lysis buffer. After the column had been washed with 10 column volumes of the lysis buffer, the bound protein was eluted with 3 column volumes of the same buffer containing 1 M NaCl. The eluted protein containing TP2 (>95% pure) was desalted and concentrated.

*In Vitro Phosphorylation of TP2, V8 Protease Cleavage, and Phosphoamino Acid Analysis.* In vitro phosphorylation of TP2 was carried out at room temperature in 20 µL of kinase buffer [20 mM Tris-HCl (pH 7.5), 20 mM NaCl, 1 mM benzamidine, 10 mM MgCl<sub>2</sub>, and 0.2 mM PMSF]. Four micrograms of either wild-type or mutant TP2 was incubated with 1.5 µL (1.5 µg) of the SRN extract in the presence of 100 µM cold ATP and 10 µCi of [ $\gamma$ -<sup>32</sup>P]ATP (3000 Ci/mmol, BARC, Mumbai, India) for 30 min. Inhibitors and/or activators were added prior to the addition of nuclear extract. In the case of purified PKA (New England Biolabs, Promega), 2 units of the enzyme was used to phosphorylate the same amount of TP2. The reaction was stopped by adding equal volume of 2× SDS gel loading buffer followed by boiling at 95 °C for 5 min. The reaction mixtures were separated on 15% SDS–PAGE (28), stained with Coomassie brilliant blue R, destained, dried, and autoradiographed. Alternatively, the reaction was stopped by adding trichloroacetic acid to a final concentration of 25%. The precipitate was washed with acidified acetone followed by ice-cold acetone, dissolved in 20 µL of ammonium acetate buffer (50 mM, pH 4.0), and subjected to V8 protease (from *Staphylococcus*, Sigma) digestion for 12–16 h at 37 °C, and the products were separated on 15% acid–urea–PAGE (29), stained with amido black, destained, dried, and autoradiographed.

For phosphoamino acid analysis, 10 µg of in vitro-labeled TP2, digested with V8 protease, was separated on a 15% acid–urea–polyacrylamide gel, and the peptides were electrophoretically transferred onto a PVDF membrane using the acid–urea buffer system as described by Wang et al. (30). The membrane was then dried on Whatman 3MM paper and autoradiographed. The radioactive spot was excised out and subjected to phosphoamino acid analysis as described by Kamps and Sefton (31). Briefly, the Immobilon PVDF membrane containing the phosphorylation band was excised, rewetted for 30 s in methanol, washed several times in water, and placed in a 1.5 mL microfuge tube. To this was added 200 µL of 7.5 N HCl; the lid was secured, and the tube was incubated at 110 °C for 3 h. After hydrolysis, it was spun at 14 000 rpm for 5 min and the supernatant was transferred to a new microfuge tube. The HCl was evaporated by placing the sample in a desiccator along with NaOH pellets and anhydrous calcium chloride to absorb the HCl vapors and moisture, respectively. The residue was resuspended in 50 µL of water and dried in a centrifugal vacuum concentrator

(Savant Speedvac). This was repeated three times to remove the acid. The residue was then dissolved in the chromatography buffer [isobutyric acid and 0.5 N ammonium hydroxide (5:3, v/v)], mixed with all the three phosphoamino standards (3  $\mu$ g each of P-serine, P-threonine, and P-tyrosine) (Sigma), and spotted onto a cellulose thin layer plate (Merck). The phosphoamino acids were separated by one-dimensional chromatography using isobutyric acid and 0.5 N ammonium hydroxide (5:3, v/v) as the solvent system (32). The standard phosphoamino acids were detected by 0.25% ninhydrin spraying and radiolabeled amino acids by autoradiography.

**In Vivo Labeling of Testicular Proteins.** The method for in vivo labeling of testicular proteins was adopted from Kundu et al. (33). The rats that were used were 60-day-old Wistar rats which were anesthetized using diethyl ether. They were then intratesticularly injected with carrier free [ $^{32}$ P]orthophosphate (500  $\mu$ Ci/testicle). The radioactive phosphoric acid was neutralized with 100 mM sodium bicarbonate, and a total volume of 100  $\mu$ L was injected into each testis. After 4 h, the animals were sacrificed, and sonication resistant nuclei were then isolated from the testes as described above. Salt extract of SRN was prepared by extracting with 1 mL of 20 mM Tris-HCl (pH 7.5), 1 M NaCl, 0.2 mM PMSF, and 5 mM EDTA. The pellet was homogenized for ~5 min with a homogenizer on ice to extract the proteins, and 100  $\mu$ L of supernatant was subjected to trichloroacetic acid precipitation. An aliquot of the precipitate was analyzed on a 15% acid-urea-polyacrylamide gel and autoradiographed. The remainder of the precipitate was dissolved in 40  $\mu$ L of 50 mM ammonium acetate buffer (pH 4.0) and digested with V8 protease at 37 °C for 12–16 h. The digested sample was analyzed on a 15% acid-urea-polyacrylamide gel along with recombinant TP2.

**Purification of Recombinant GST-2K.** Plasmid GST-2K (Pharmacia) carrying GST having a consensus PKA phosphorylation site at the C-terminus of the protein was induced in *E. coli* DH5 $\alpha$  cells with IPTG. The induced protein was purified in a single step using glutathione-Sepharose 4B (Pharmacia) according to the manufacturer's protocol.

**Purification of Recombinant Phosphorylated TP2.** Phosphorylated TP2 used for CD experiments was purified using the heparin-agarose column to remove the kinase. Recombinant TP2 was phosphorylated in vitro with PKA in the presence of 0.5  $\mu$ Ci of [ $\gamma$ - $^{32}$ P]ATP and 100  $\mu$ M ATP as described above and loaded onto the heparin-agarose column which was pre-equilibrated with buffer containing 50 mM Tris HCl (pH 8.0), 300 mM NaCl, 10 mM  $\beta$ -mercaptoethanol, and 0.2 mM PMSF. The column was washed with 5 volumes of the same buffer or until negligible radioactivity was detected in the wash. The phosphorylated TP2 was eluted from the column with the same buffer containing 1 M NaCl. The extent of phosphorylation of recombinant TP2 was found to be more than 98% as demonstrated by densitometric analysis of an acid-urea-PAGE gel (29) which showed differences in the mobility of phosphorylated and unphosphorylated TP2.

**Circular Dichroism Spectroscopy.** Circular dichroic spectra of TP2 nucleoprotein complexes were recorded in a JASCO (J-20C) spectropolarimeter from 320 to 220 nm according to the method of Kundu and Rao (8). Each spectrum is an average of three scans. All the circular dichroic spectra of DNA-protein complexes were recorded at room temperature

```

1      10      20      30
MDTKMQSLPTTHPHPHSSSRPQSHTNNQCACSHHCRSC
40      50      60      70
SQAGHPSSSSSPSPGPPTKHPKTPMHSRYSRSPSRERG
80      90      100     110
SCPKNRKTLE↑GKVSKRKAVRRRRKTRHAKRRSSGRRYK

```

FIGURE 1: cDNA-derived amino acid sequence of rat TP2. The arrow indicates the unique glutamic acid at position 86 which has been exploited in generating the N-terminal and C-terminal fragments following V8 protease digestion.

in a buffer containing 10 mM Tris-HCl (pH 7.5), 20 mM NaCl, and 10  $\mu$ M ZnSO $_4$ . The complexes were formed by adding buffer, DNA, and finally the protein (phosphorylated or unphosphorylated TP2). The reaction mixtures were incubated for 10 min, for each addition of an aliquot of protein sample. The synthetic polynucleotide poly(dG-dC)·poly(dG-dC) (Pharmacia) was dissolved in TE and dialyzed against CD buffer overnight before use. To determine the effect of dephosphorylation of the DNA-TP2 complex on DNA condensation, the complexes were treated with calf intestinal phosphatase (4 units/ $\mu$ g of TP2 in the complex) and incubated for 30 min at room temperature (in the cuvette), and subsequently, the CD spectrum was recorded. The change in molar ellipticity observed at 270 nm was plotted as a function of the protein:DNA ratio (moles of protein per base pair).

**In Vitro Kinase Reaction of the Protein-DNA Complex.** Protein-DNA complexes were allowed to form first in a buffer containing 20 mM Tris-HCl (pH 7.5), 20 mM NaCl, 1 mM benzamidine, 10 mM MgCl $_2$ , 0.2 mM PMSF, and 10  $\mu$ M ZnSO $_4$ . In a typical 20  $\mu$ L reaction mixture, increasing amounts of TP2 were incubated with either rat oligonucleosomal DNA (0.8–2.0 kb) or poly(dG-dC)·poly(dG-dC) for 10 min at room temperature. The kinase reaction was initiated by simultaneous addition of PKA (0.3 unit), 100  $\mu$ M ATP, and 0.5  $\mu$ Ci of [ $\gamma$ - $^{32}$ P]ATP. The reaction was stopped after 30 min by adding an equal volume of 2 $\times$  SDS loading buffer followed by boiling at 95 °C for 5 min. The proteins were separated on a 15% SDS-PAGE gel stained with Coomassie brilliant blue R, destained, dried, and autoradiographed. GST-2K protein was used as a negative control to check the nonspecific effect of DNA on protein kinase A activity. A theoretical analysis of the potential phosphorylation sites present in TP2 was carried out using the website program NetPhos 2.0 prediction Server at [www.cbs.dtu.dk/services/NetPhos](http://www.cbs.dtu.dk/services/NetPhos).

## RESULTS

**Identification of the Phosphorylation Site in TP2.** The amino acid sequence of rat TP2 is shown in Figure 1, and the predicted phosphorylation sites as revealed by a computer-assisted search are given in Table 1. There are several potential sites for various protein kinases such as CaMI, CKI, GSK3, p34cdc2, p70s6k, PKA, PKC, and PKG. It is, therefore, very pertinent to identify the sites that are phosphorylated in vivo in the cell type wherein this protein is expressed during spermiogenesis. TP2 is transcribed during early stages of spermiogenesis, and the mRNA is stored in the cytoplasm as mRNP which is translationally activated



Table 1: Predicted Phosphorylation Sites in TP2

protein kinase	potential phosphorylation site	motif
CaMI	S23	RPQSHTN
	S39	RSCSQAG
	T101	RKRTHRA
	S109	RRSSGRR
CKI	S7	TKMQSLPT
	S23	SRPQSHTN
	S49	SSSSPSP
	S65	TPMHSRYS
GSK3	S73	SRPSHRG
	S19	HSSSRPQS
	S45	GHPSSSSS
	T61	HPKTPMSH
p34cdc2	S73	SRPSHRGS
	S68	SRYSPSR
	T101	RRRKRTHRA
	S23	RPQSHTN
p70s6k	S39	RSCSQAG
	S68	RYSPPSR
	S73	RPSHRG
	S77	RGSCPCK
PKA	T84	RKTLEG
	T101	RKRTHRA
	S109	RRSSGRR
	S18	PHSSSRP
PKC	S73	SRPSHRG
	S90	GKVSKRK
	T101	RKRTHRA
	S108	RRSGRR
PKG	S109	RRSSGRR
	T101	RRRKRTHRA
	S109	KRRSSGRR

during late stages (3). As mentioned in the introductory section, this period of spermiogenesis is not easily amenable for a detailed biochemical analysis of phosphorylation by cell culture methods. Alternatively, we surmised that since all the transition proteins (TP1, TP2, and TP4) can be isolated from SRN which can be prepared in a highly pure form, the salt extract of SRN could be used for our phosphorylation studies to identify the sites that can be phosphorylated in TP2 by this extract in vitro and also the nature of protein kinase involved in this phosphorylation reaction. Recombinant TP2 expressed in *E. coli* was used in all the phosphorylation studies. Figure 2A shows the Coomassie blue-stained pattern of SDS-PAGE whose autoradiogram is shown in Figure 2B. It is clear from the figure that TP2 is very efficiently phosphorylated by the SRN extract (lane 2) that was not stimulated by calcium ions (lane 3). There was a small but significant stimulation (1.5-fold) by 100  $\mu$ M cyclic AMP (lane 4). There is a single Cdc2 kinase phosphorylation site (<sup>68</sup>SPSR<sup>71</sup>). However, S68A mutant TP2 was equally phosphorylatable (lane 5), indicating that Cdc2 kinase is not involved in phosphorylation of TP2 by the SRN extract. The lack of stimulation by calcium ions and a marginal stimulation by cAMP suggested to us that probably protein kinase A may be involved in phosphorylation of TP2 by the SRN extract. There are eight potential sites in TP2, which can be phosphorylated by protein kinase A (Table 1). To narrow down the range of locations of the phosphorylation site, we made use of the single glutamate residue at position 86 to generate the N-terminal two-third and C-terminal one-third fragments of TP2 after cleavage with V8 protease. The in vitro-phosphorylated recombinant TP2 was cleaved with V8 protease, and the two fragments were

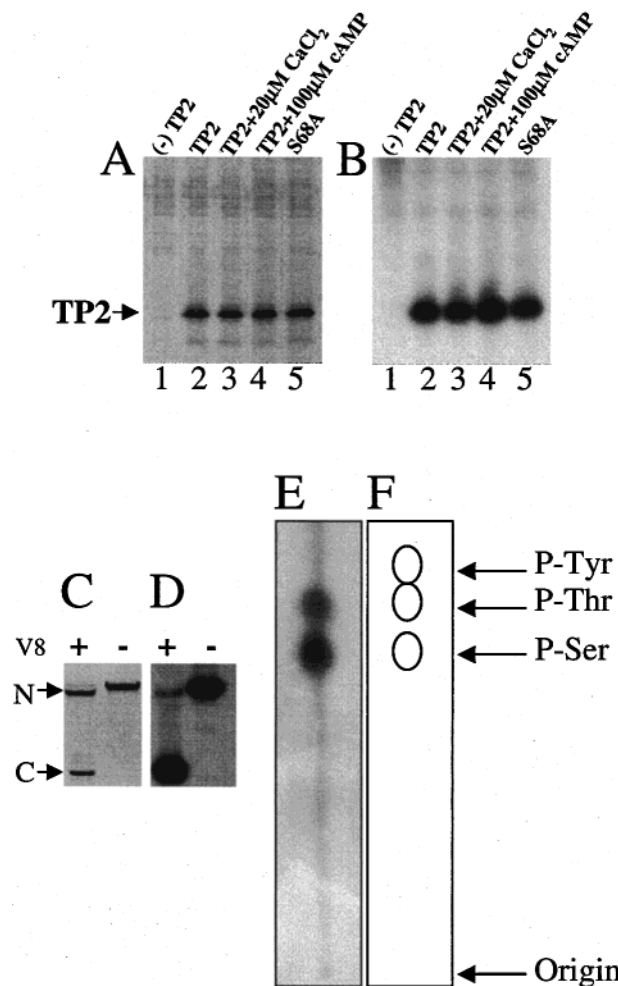
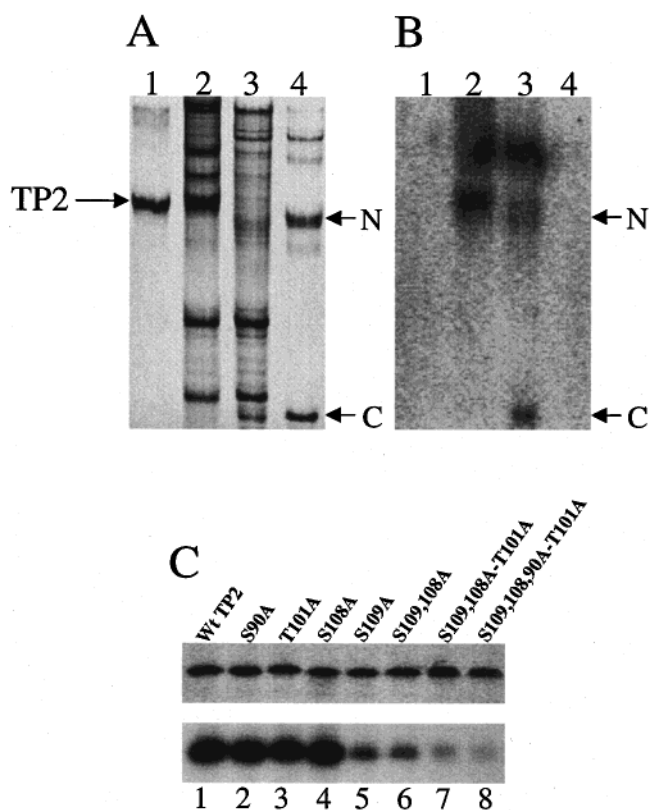


FIGURE 2: (A) In vitro phosphorylation of TP2 with SRN extract. Recombinant TP2 (4  $\mu$ g) was incubated with SRN extract (approximately 1.5  $\mu$ g of protein) in the presence of 10  $\mu$ Ci of [ $\gamma$ -<sup>32</sup>P]ATP as described in Experimental Procedures. The proteins were separated via 15% SDS-PAGE, stained with Coomassie blue, dried, and autoradiographed: lane 1, SRN extract alone; lane 2, recombinant TP2 and SRN extract; lane 3, recombinant TP2 and SRN extract in the presence of 20  $\mu$ M CaCl<sub>2</sub>; lane 4, recombinant TP2 and SRN extract in the presence of 100  $\mu$ M cAMP; and lane 5, recombinant S68A mutant TP2 and SRN extract. (B) Autoradiogram of panel A. (C) Localization of phosphorylation sites in TP2. Recombinant TP2 was phosphorylated with SRN extract in the presence of [ $\gamma$ -<sup>32</sup>P]ATP, cleaved with V8 protease, separated via 15% acid-urea-PAGE, and stained with amido black. (D) Autoradiogram of panel C. (E) Phosphoamino acid analysis of the C-terminal domain of TP2. The phosphorylated and V8 protease-cleaved TP2 was transferred from an acid-urea-PAGE gel to the PVDF membrane. The C-terminal radioactive peptide was hydrolyzed with 5.7 N HCl as described in Experimental Procedures. The hydrolysate was separated by one-dimensional thin-layer chromatography on a cellulose plate with isobutyric acid and 0.5 N ammonium hydroxide (5:3, v/v) as the solvent and analyzed by autoradiography. (F) The positions denoted with arrows are those of the cold phosphoamino acid standards as observed after ninhydrin staining.

separated on acid-urea-PAGE and subjected to autoradiography. The results presented in panels C and D of Figure 2 show that the major phosphorylation site is localized to the C-terminal third of TP2, although a faint signal was observed in the N-terminal fragment of TP2. The radioactive C-terminal fragment of TP2 was subjected to phosphoamino acid analysis wherein both phosphoserine and phosphothreonine were detected in a ratio of 6:1 (Figure 2E)



**FIGURE 3:** (A and B) Distribution of in vivo phosphorylation sites in TP2. (A) Carrier free [ $^{32}\text{P}$ ]orthophosphate (500  $\mu\text{Ci}$ /testicle) was injected intratesticularly, and the salt extractable proteins were prepared from sonication resistant nuclei as described in Experimental Procedures. An aliquot was digested with V8 protease, and the proteins were separated via 15% acid-urea-PAGE, stained with amido black, dried, and autoradiographed: lane 1, recombinant TP2; lane 2, 1 M NaCl extract of SRN after in vivo labeling with [ $^{32}\text{P}$ ]orthophosphoric acid; lane 3, 1 M NaCl extract after cleavage with V8 protease; and lane 4, recombinant TP2 after cleavage with V8 protease. N denotes the N-terminal fragment and C the C-terminal fragment of TP2. (B) Autoradiogram of panel A. (C) Effect of serine and threonine mutations on the phosphorylatability of TP2 by the SRN extract. The serine and threonine mutants (single and multiple) were generated by the PCR method as described recently (25). The recombinant wild-type and mutant TP2s were phosphorylated with the SRN extract, separated on SDS-PAGE, stained with Coomassie blue, dried, and autoradiographed: (top panel) stained pattern and (bottom panel) autoradiogram; lane 1, wild-type TP2; lane 2, S90A mutant; lane 3, T101A mutant; lane 4, S108A mutant; lane 5, S109A mutant; lane 6, S109,108A double mutant; lane 7, S109,108A-T101A triple mutant; and lane 8, S109,108,90A-T101A quadruple mutant.

as determined by counting the radioactivity associated with these two spots.

The experiments described above were carried out in vitro with recombinant TP2 by using the salt extract of sonication resistant nuclei as the source of protein kinases. An obvious question that needs to be addressed is the phosphorylation status of TP2 in vivo. For this purpose, the testicular proteins were labeled with [ $^{32}\text{P}$ ]orthophosphate as mentioned in Experimental Procedures. Sonication resistant nuclei were prepared, and the proteins were extracted with 1 M NaCl. They were separated on acid-urea-PAGE and subjected to autoradiography. Among several proteins that are present in this salt extract, TP2 is a major phosphorylated band (Figure 3B, lane 2). After cleavage with V8 protease, the major phosphorylation site was localized to the C-terminal

third of TP2 with a minor phosphorylation site in the N-terminal two-thirds of TP2 (lane 3). This result, therefore, confirms the observations made above on in vitro phosphorylation experiments with the SRN extract, which gave the indication that in vitro phosphorylation mimics the in vivo situation, and hence, we proceeded for further characterization.

To localize the phosphorylation site in the C-terminal third of TP2, we resorted to site-directed mutagenesis. In the C-terminal region, serine residues are present at positions 90, 108, and 109 and threonine is present at position 101. All these residues were changed to alanine as single mutants as well as in combination, which were then used for the phosphorylation reaction using the SRN extract. The top panel in Figure 3C shows the Coomassie blue-stained pattern, while the bottom panel shows the autoradiographic pattern. Mutations at Ser 90 and Ser 108 had no effect on the phosphorylation of TP2 (lanes 2 and 4), while mutation of Ser 109 resulted in a drastic decrease in the phosphorylatability of TP2 (lane 5). The level of residual phosphorylation observed with S109A (lane 5) was further reduced in the triple mutant S109,108A-T101A, indicating that this residual phosphorylation was probably taking place at T101. This is also evident in lane 3, wherein there was a small but significant decrease in the phosphorylatability of the T101A mutant compared to wild-type TP2 (lane 1). The phosphorylation observed in lane 8 of the S109,108A-T101A mutant might represent a weak phosphorylation site in the N-terminus, which was also observed in the V8 protease-derived N-terminal fragment (Figure 3B). In this communication, we have not addressed the question of identification of this minor phosphorylation site in the N-terminal fragment of TP2. Thus, the results presented in Figure 3C demonstrate that Ser 109 and Thr 101 represent a strong and a weak phosphorylation site, respectively, in TP2. This also agrees with the phosphoamino acid analysis (Figure 2C) wherein the ratio of P-Ser to P-Thr was found to be 6:1.

**Protein Kinase A Is Involved in Phosphorylation of TP2.** Serine 109 and threonine 101 happen to be a part of overlapping peptide sequences that can be phosphorylated by protein kinase A, protein kinase G, and protein kinase C. To identify which of these three kinases present in the SRN extract is responsible for phosphorylation at serine 109 and threonine 101, we carried out phosphorylation experiments with specific inhibitors. The results of these experiments are shown in Figure 4A. EGTA, a specific chelator of calcium, at 2 mM did not affect phosphorylation of TP2 (lane 2), indicating protein kinase C is probably not involved in phosphorylation of TP2. This was further strengthened by the observation that bisindolylmaleimide (0.5  $\mu\text{M}$ ), a specific inhibitor of protein kinase C, had no effect on the extent of phosphorylatability of TP2 by the SRN extract (lane 3). Thus, it is very unlikely that protein kinase C is involved in the phosphorylation of serine 109 and threonine 101 of TP2. On the other hand, staurosporine (lane 4), a general inhibitor of serine/threonine kinase, and the protein kinase A inhibitor (PKI) peptide (lane 5) resulted in almost near complete inhibition equivalent to that observed in the serine and threonine mutants (lanes 6 and 7). These results strongly suggest that protein kinase A in the SRN extract is responsible for phosphorylating TP2. This conclusion was

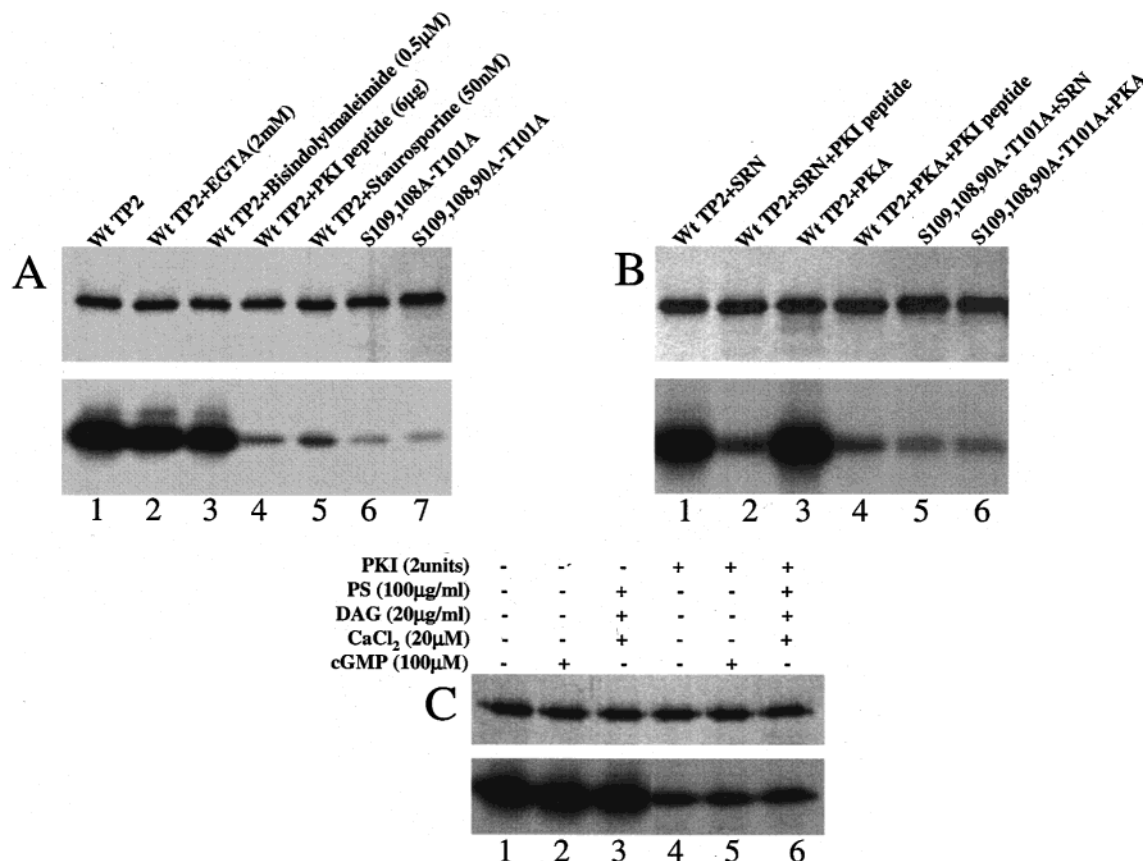


FIGURE 4: (A) Effect of inhibitors on phosphorylation of TP2 by the SRN extract. Phosphorylation of wild-type recombinant TP2 was carried with the SRN extract in the presence of various inhibitors: (top panel) Coomassie blue-stained pattern and (bottom panel) autoradiogram; lane 1, wild-type TP2 without any inhibitor; lane 2, wild-type TP2 with 2 mM EDTA; lane 3, wild-type TP2 with 0.5  $\mu$ M bisindolylmaleimide (specific inhibitor of protein kinase C); lane 4, wild-type TP2 with 50  $\mu$ M staurosporine (general serine and threonine kinase inhibitor); lane 5, wild-type TP2 with 6  $\mu$ g of protein kinase A inhibitor (PKI) peptide; lane 6, S109,108A-T101A triple TP2 mutant; and lane 7, S109,108,90A-T101A TP2 quadruple mutant. (B) Phosphorylation of TP2 by purified protein kinase A. Wild-type and mutant TP2 were phosphorylated with the SRN extract or purified protein kinase A: (top panel) Coomassie blue-stained pattern and (bottom panel) autoradiogram; lane 1, wild-type TP2 with the SRN extract; lane 2, wild-type TP2 with the SRN extract in the presence of 6  $\mu$ g of protein kinase A inhibitor (PKI) peptide; lane 3, wild-type TP2 with purified protein kinase A (2 units); lane 4, wild-type TP2 with purified protein kinase A in the presence of 6  $\mu$ g of protein kinase A inhibitor (PKI) peptide; lane 5, S109,108,90A-T101A quadruple mutant with the SRN extract; and lane 6, S109,108,90A-T101A quadruple mutant with purified protein kinase A. (C) Phosphorylation of TP2 in the presence of other cofactors: (top panel) SDS-PAGE pattern and (bottom panel) autoradiogram; lane 1, TP2 with the SRN extract; lane 2, TP2 with cGMP; lane 3, TP2 with phosphatidylserine, diacylglycerol, and CaCl<sub>2</sub>; lane 4, TP2 with PKI; lane 5, TP2 with cGMP and PKI; and lane 6, TP2 with phosphatidylserine, diacylglycerol, CaCl<sub>2</sub>, and PKI. In this experiment, PKI was from New England Biolabs.

further corroborated by the results obtained from the experiments described in Figure 4B. Purified protein kinase A was able to phosphorylate TP2 (lane 3) which was inhibited by the inhibitor peptide (lane 4). At the same time, purified protein kinase A did not phosphorylate the mutant TP2 (lane 6). As already mentioned above, S109 and T101 happen to be part of the peptide sequence that can be phosphorylated by cGMP-dependent protein kinase. To rule out the possibility of the involvement of cGMP-dependent protein kinase, we carried out experiments *in vitro* by adding cGMP to the SRN extract. The results presented in Figure 4C show that 100  $\mu$ M cGMP did not stimulate the phosphorylation observed with the SRN extract alone (lane 2). Furthermore, cGMP in the presence of PKI (New England Biolabs) did not result in an increase in the extent of phosphorylatability over and above that of PKI alone (lanes 4 and 5). We also carried out additional experiments to rule out completely the involvement of protein kinase C in the phosphorylation of TP2. In Figures 2 and 4A, we show that calcium and EGTA had no effect on the phosphorylatability of TP2. We also added to the SRN extract all the cofactors, calcium ions,

phosphatidylserine (PS), and diacylglycerol (DAG), that are necessary for the protein kinase C reaction. However, even in the presence of these cofactors, there was no stimulation of phosphorylation observed with the SRN extract alone (lanes 1 and 3). More importantly, in the presence of these cofactors, PKI inhibited the phosphorylation reaction (lane 6) in a manner equivalent to that observed with PKI in the absence of these cofactors. Thus, these experiments unequivocally demonstrate the involvement of protein kinase A in the phosphorylation of TP2.

*The TP2-DNA Complex Is Not Phosphorylatable.* Since TP2 is a DNA-binding protein, an obvious question that arises at this point is whether phosphorylation of TP2 occurs before its deposition on the chromatin or on chromatin prior to its displacement by protamines. This question is relevant particularly since the major phosphorylation sites are located in the C-terminal third of the protein containing predominantly the basic amino acids. We point out here the fact that Greene et al. (21) concluded previously that TP2 is phosphorylated immediately after its synthesis from their *in vivo* <sup>32</sup>P labeling experiments. In this study, we have asked



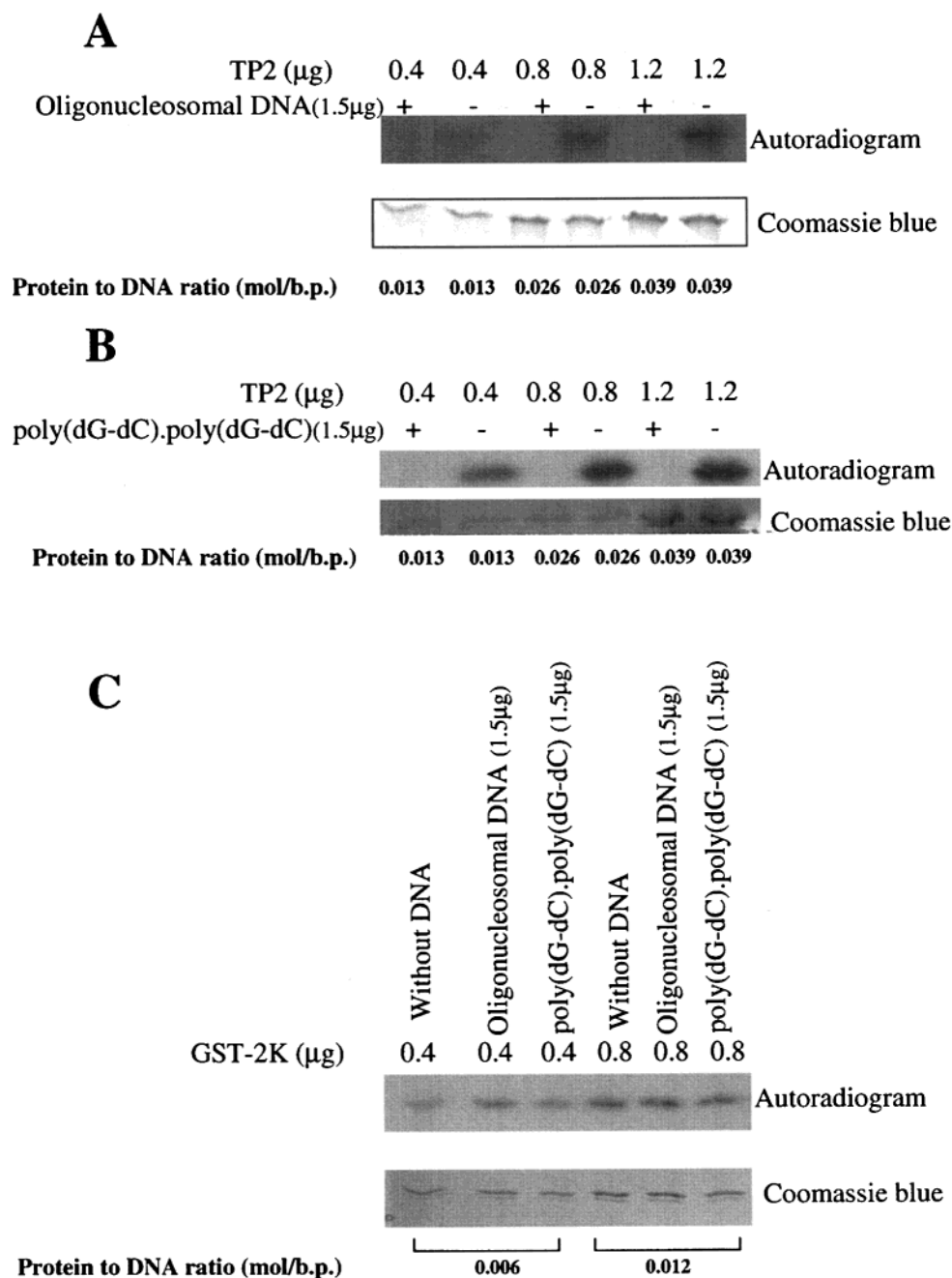


FIGURE 5: Phosphorylation of TP2 in the context of the TP2–DNA complex. Increasing amounts of wild-type TP2 were phosphorylated using PKA (0.3 unit) after preincubation with 1.5  $\mu\text{g}$  of oligonucleosomal DNA (A) or poly(dG-dC)·poly(dG-dC) (B). As a control, GST-2K was incubated with PKA (0.3 unit) under similar conditions with either the oligonucleosomal DNA complex or the poly(dG-dC)·poly(dG-dC) complex (C): (top panel) autoradiogram and (bottom panel) Coomassie blue-stained pattern.

whether TP2 is phosphorylatable in a DNA–protein complex. In this series of experiments, increasing amounts of recombinant TP2 were mixed with a constant amount of either oligonucleosomal DNA (Figure 5A) or poly(dG-dC)·poly(dG-dC) (Figure 5B) and then incubated with PKA and [ $\gamma$ - $^{32}\text{P}$ ]ATP. The ratios of protein to DNA that were used were 0.013, 0.026, and 0.039 (moles per base pair) which were the same ratios used subsequently in circular dichroism experiments. The results presented here clearly show that TP2 was not phosphorylatable when complexed with either of the two types of DNA. At all ratios of protein to DNA, there was no increase in the absorbance at 400 nm, indicating that the complexes being studied were soluble in nature. The ratios of TP2 to DNA used here correspond to  $r^{+/-}$  ratios

[moles of total positive charge (lysine plus arginine) per base pair] of 0.351, 0.702, and 1.053, respectively. We have found that the nucleoprotein complexes come out of solution only at an  $r^{+/-}$  ratio of 1.2, as also has been found with protamines (19), and the complexes remain soluble at either side of this electroneutrality (4, 34). It may be worth noting here that there are a total of 11 lysines and 16 arginines in TP2, among which 16 basic residues are present in the C-terminal third while only 11 residues are spread out in the N-terminal two-thirds of the molecule which also contains the zinc fingers. In a control experiment, both oligonucleosomal DNA and poly(dG-dC)·poly(dG-dC) did not have any effect on the phosphorylatability of GST-2K (containing the PKA site), indicating that the effect observed with TP2 is a specific



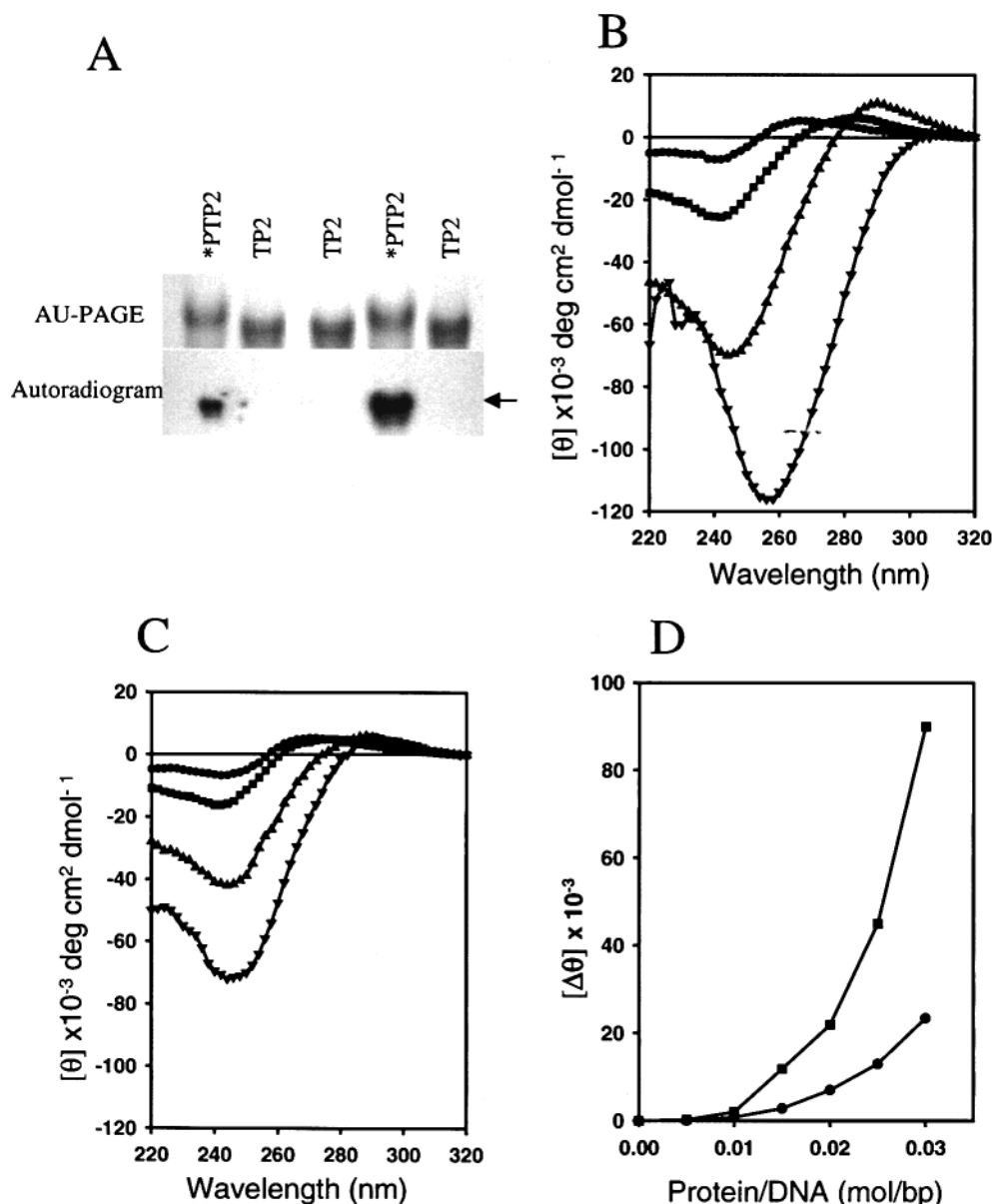


FIGURE 6: Effect of phosphorylation on the DNA condensation property of TP2. (A) Acid-urea-PAGE showing the differences in mobility between TP2 and PTP2. Equal amounts of protein (4  $\mu$ g) were loaded in the indicated order. The top panel shows the proteins stained with amido black, while the bottom panel shows the autoradiogram of the same showing the phosphorylated TP2 as indicated. (B and C) Circular dichroism spectroscopy of poly(dG-dC)·poly(dG-dC) with increasing concentrations of TP2 and PTP2, respectively: (●) DNA alone, (■) protein:DNA ratio of 0.01 (moles of protein per base pair), (▲) protein:DNA ratio of 0.02 (moles of protein per base pair), and (▼) protein:DNA ratio of 0.03 (moles of protein per base pair). (D) Comparison of DNA condensation properties of TP2 and PTP2. Ellipticity changes observed at 270 nm in panels B and C upon binding to TP2 and pTP2, termed as  $\Delta\theta$ , are plotted as a function of the protein:DNA ratio (moles of protein per base pair): (■) TP2 and (●) PTP2.

one and not a nonspecific effect on protein kinase A (Figure 5C).

**Phosphorylation of TP2 Affects DNA Condensation.** TP2 is also a DNA condensing protein showing a sequence preference for alternating GC-rich sequence (8). Since phosphorylation occurs in the C-terminal region, containing predominantly basic amino acids, we were curious to determine the effect of phosphorylation of TP2 on its DNA condensing property. For this purpose, we prepared phosphorylated TP2 (PTP2) by incubating recombinant TP2 with protein kinase A in the presence of cold ATP and a trace amount of [ $\gamma$ -<sup>32</sup>P]ATP. PTP2 was purified as described in Experimental Procedures using the heparin-agarose column. The extent of phosphorylation was checked by electrophoresis on an acid-urea-PAGE gel (Figure 6A). The

phosphorylated protein had a slightly retarded mobility compared to unphosphorylated TP2. A densitometric scan revealed that more than 98% of TP2 was in the phosphorylated state. Subsequently, the condensation properties of both TP2 and PTP2 were determined by circular dichroism spectroscopy (8) using poly(dG-dC)·poly(dG-dC) as the substrate (Figure 6B,C). The condensation parameter  $\Delta\theta$ , observed at 270 nm, is plotted as a function of increasing protein to DNA ratio in terms of moles of protein per base pair in Figure 6D. It is clear that there is an almost 70–80% decrease in the condensation property of PTP2 at similar protein to DNA ratios as compared to TP2. Thus, phosphorylation seems to have a major effect on TP2-mediated DNA condensation. To rule out the possibility that the effect of phosphorylation on DNA condensation is not due to a

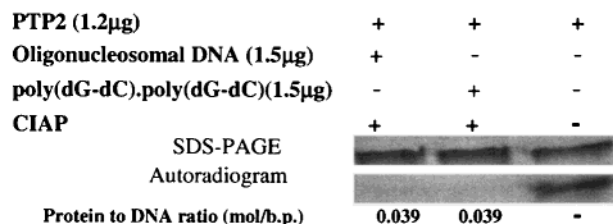
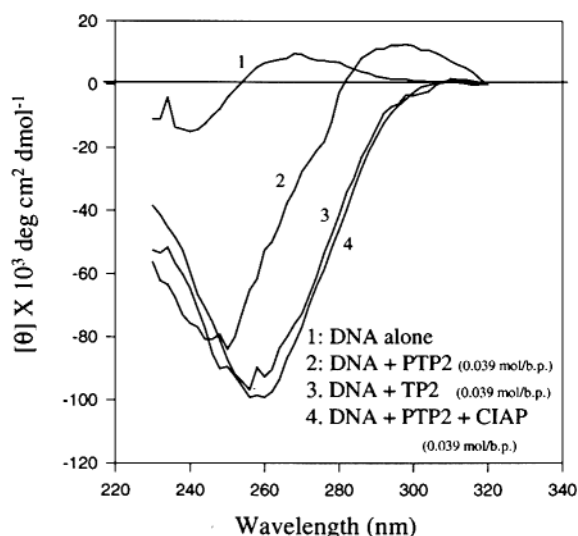
**A****B**

FIGURE 7: (A) Dephosphorylatability of PTP2–DNA complexes. PTP2 was preincubated with either oligonucleosomal DNA or poly(dG-dC)·poly(dG-dC), as indicated, and treated with CIP (6 units/ $\mu$ g of PTP2) for 30 min. The top panel shows the autoradiogram, while the lower panel shows the SDS–PAGE profile of the autoradiogram. (B) Effect of dephosphorylation of PTP2 on DNA condensation. Circular dichroism spectroscopy of poly(dG-dC)·poly(dG-dC) with TP2, PTP2, and PTP2 and poly(dG-dC)·poly(dG-dC) treated with CIP at the same ratio of moles of protein per base pair (0.039).

lack of DNA binding, we carried out a gel mobility shift assay using a human CpG island sequence (9) with both phosphorylated and unphosphorylated TP2. There was no difference observed in the binding ability between the TP2 and PTP2 (data not shown).

We were then curious to know whether dephosphorylation of PTP2 within the protein–DNA complex will restore the condensation property of TP2. For this purpose, we had to first demonstrate that calf intestinal phosphatase does dephosphorylate PTP2 when complexed with DNA. As can be seen in Figure 7, CIP did dephosphorylate PTP2 when complexed with either oligonucleosomal DNA or poly(dG-dC)·poly(dG-dC). Subsequently, we recorded the CD spectra of poly(dG-dC)·poly(dG-dC) when it was complexed to PTP2 (moles per base pair ratio equivalent to an  $r^{+/-}$  of 1.05). As can be seen in Figure 7B, there was a reduction in the level of DNA condensation in comparison with that of unphosphorylated TP2 ( $\Delta\theta$  at 270 nm). We then added CIP to the PTP2–DNA complex in the CD cuvette and recorded the CD spectrum after 30 min. As is evident from Figure 7B, the phosphatase treatment resulted in the restoration of the condensation property of TP2. In a control experiment, we observed that CIP alone did not have any effect

on the CD spectrum of poly(dG-dC)·poly(dG-dC) (data not shown).

## DISCUSSION

This investigation deals with a detailed analysis of phosphorylation of spermatidal protein TP2. The results of the experiments presented here have clearly demonstrated that there are at least three phosphorylation sites in TP2. They are (a) a major phosphorylation site at serine 109, (b) a minor phosphorylation site at threonine 101, and (c) a minor phosphorylation site in the N-terminal V8 protease-derived fragment, and (d) the phosphorylation of serine 109 and threonine 101 is mediated by protein kinase A. Since the relative phosphorylation of the C-terminal and N-terminal fragments observed *in vivo* is similar to that observed when recombinant TP2 was incubated with the SRN extract, we presume that the results obtained with the SRN extract probably reflect the *in vivo* situation. In this investigation, we have not attempted to characterize the minor phosphorylation site in this N-terminal fragment, although the experiment with S68A rules out the possibility of Cdc2 kinase in the phosphorylation of TP2.

As mentioned in the introductory section, Green et al. (21) had observed that TP2 is rapidly phosphorylated *in vivo* in both rat and mouse testis, although they did not characterize the site(s) of phosphorylation. On the basis of the occurrence of several SP residues in TP2, they had predicted that Cdc2 kinase might be involved in the phosphorylation of TP2. However, our results with the S68A mutant (target sequence, <sup>68</sup>SPSR<sup>71</sup>) clearly rule out the involvement of Cdc2 kinase. On the other hand, Levesque et al. (23) had observed that both recombinant TP1 and TP2 are phosphorylated *in vitro* by purified protein kinase C, while purified protein kinase A phosphorylated only TP1 but only weakly TP2. Our results contradict these results since we have clearly demonstrated that it is protein kinase A that is present in the SRN extract which is responsible for phosphorylation of serine 109 and threonine 101. We have even demonstrated that these sites are phosphorylated with purified protein kinase A. The reason for this discrepancy is not clear at present. However, we point out one major difference between our experiments and theirs. They have used pH 6.4 in their phosphorylation studies with protein kinase A, while our assay was carried out at pH 7.5. They have used only purified kinases in their studies, while we have used the SRN extract in most of the studies and further corroborated these results with purified protein kinase A. The observation that TP1 can be phosphorylated by both protein kinases A and C does not agree with the results of Green et al. (21), who observed that TP1 is not phosphorylated *in vivo*.

Although the results presented here clearly show the involvement of PKA in the phosphorylation of TP2, they do not provide direct evidence for its involvement *in vivo*. For this purpose, one needs to address this question at the round spermatid level, the germ cells wherein the TP2 gene is expressed in a tissue specific and stage specific manner. The lack of a well-established culture system for the round spermatids has made this study not feasible so far. We are at present standardizing the conditions for maintaining round spermatids in culture and subsequent DNA transfections. This model system will be used in future to examine the *in vivo*

phosphorylation sites of TP2 and the involvement of PKA, the results of which will be presented elsewhere.

There was only an ~1.5-fold stimulation of phosphorylation of TP2 by the SRN extract in the presence of cAMP, suggesting that most of the PKA is already in the activated form. Protein kinase A is an important component of the signal transduction pathway, and recently, it has been demonstrated that its catalytic subunit is targeted to different organelles through specific association of the regulatory subunit with anchoring proteins called "A-kinase-anchoring proteins" (AKAPs) (35, 36). This kind of targeting is believed to narrow down its broad substrate specificity because its target recognition and/or phosphorylation sites are widely distributed in many proteins. TKAP-80, which is testis specific, is localized to the fibrous sheath of the sperm tail (37). AKAP-82 is also localized to the sperm tail and known to have a role in sperm capacitation (38, 39). Another AKAP family member, AKAP-110, is specifically expressed in round spermatids and is associated with both the sperm head and the tail (40). AKAP-95 is shown to be localized to nuclear matrix and plays a key role in chromatin condensation at mitosis (41), while mAKAP is associated with the nuclear membrane (cited in ref 35). It remains to be seen which of the AKAPs targets PKA to the nucleus of elongating spermatids.

We have also addressed another important question in the study presented here, namely, whether TP2 is phosphorylatable when present as a DNA–protein complex. This question is particularly relevant for distinguishing whether TP2 phosphorylation occurs prior to its deposition on chromatin or as a DNA–protein complex just prior to the replacement of transition proteins with protamines. The results presented here clearly showed that TP2 is not phosphorylatable when present as a DNA–protein complex (Figure 5), favoring the possibility that phosphorylation is an event prior to deposition on chromatin. An important property of TP2 is DNA condensation in a zinc-dependent manner having a preference for GC-rich sequence (8). We have also shown earlier that because of this GC-rich sequence preference, TP2 recognizes the CpG island sequence (9), and therefore, we have speculated that chromatin condensation by TP2 may be initiated at the CpG island sequences in the mammalian genome (9, 42). In this connection, it is noteworthy that phosphorylation of TP2 greatly reduces its DNA condensation ability which can be restored upon dephosphorylation of PTP2 bound to DNA (Figure 7). We have recently suggested that TP2 may be divided into two domains, one being the N-terminus having two zinc finger modules and the other C-terminal basic domain (42). Keeping this in mind, we propose a model depicting the events taking place on chromatin at the time of the appearance of TP2 (Figure 8). Immediately, after synthesis, TP2 becomes phosphorylated and this phosphorylation event temporarily inhibits the condensation property of the basic C-terminal domain, thus allowing lateral diffusion of TP2 along the chromatin to facilitate the process of its zinc finger modules searching and docking onto the GC-rich CpG island sequences. Subsequent dephosphorylation triggers the initiation of chromatin condensation. The lack of phosphorylation of the TP2–DNA complex, but the observation that dephosphorylation can occur when TP2 is bound to DNA, can be explained on the basis of the less condensed state of the

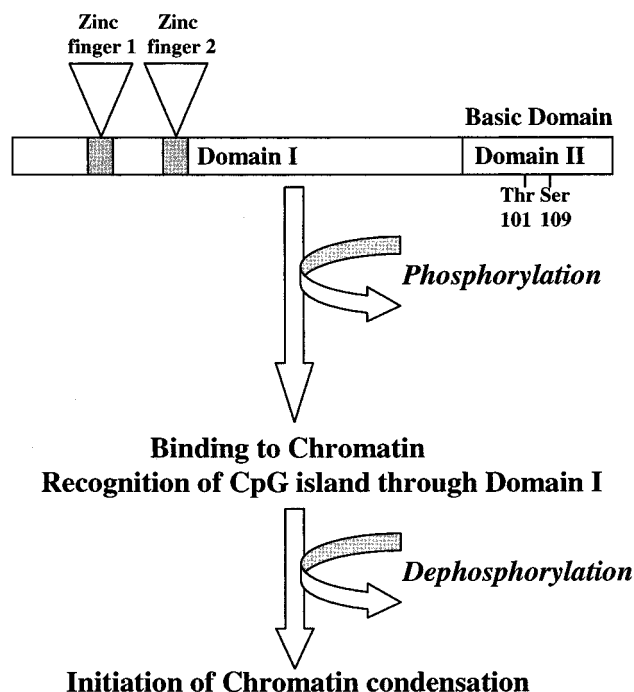


FIGURE 8: Model depicting the probable sequence of events during TP2-mediated DNA condensation.

PTP2–DNA complex as compared to the TP2–DNA complex. This proposed role of the phosphorylation–dephosphorylation cycle is very similar to the events that are visualized for protamine deposition on chromatin (20, 21). It is believed that the initial interaction of the phosphorylated protamine molecule with DNA would allow the complexes to resolve and reform, finally yielding the optimally stabilized nucleoprotamine structure. Subsequent dephosphorylation would increase the strength of the ionic interaction and further condense the sperm nucleus. The structure of the nucleoprotamine molecule has been very difficult for experimentation. A recent theoretical model proposed by Raukas and Mikelsaar (43) visualizes protamine molecules within the channels created by a DNA duplex arranged hexagonally in the  $x$ – $y$  plane. This model is quite in contrast to the earlier models in which protamine molecules were believed to be wrapped around the DNA helix (cited in ref 43). Raukas and Mikelsaar (43) also predict that the phosphorylation of protamine induces  $\alpha$ -helicity which may be necessary for optimum interaction with DNA. In this context, it would be of interest to determine the effect of phosphorylation of TP2 on the secondary structure of the C-terminal domain, which is highly basic. A recent elegant study by Wu et al. (44) has clearly demonstrated that  $\text{Ca}^{2+}$ /calmodulin-dependent protein kinase IV (Cam k4) is involved in the phosphorylation of protamine 2, and the loss of function of this gene in Cam k4<sup>−/−</sup> mice resulted in impaired exchange of basic nuclear proteins. In these mice, there is a specific loss of protamine 2 and prolonged retention of TP2 in step 15 spermatids. All these results and predictions, therefore, highlight the importance of the phosphorylation–dephosphorylation cycle in the sequence of events taking place in chromatin remodeling during the final stages of spermiogenesis. It would also be interesting to map the minor phosphorylation site(s) within the N-terminus of TP2 and to determine its possible potential to modulate the interaction of the two zinc fingers with the CpG dinucleotide. Finally,

an interesting question that has to be addressed in the future is the nature of packaging of chromatin by the transition proteins. Is the final packaging of sperm chromatin determined by the transition proteins, or is it further modified by protamines, in addition to its established role of disulfide cross-linking in compacting epididymal sperm chromatin? This question becomes relevant particularly in the context of a small percentage of mammalian sperm chromatin still retaining nucleosomal structure (45, 46).

## REFERENCES

- Meistrich, M. L. (1989) in *Histones and other Basic Nuclear Proteins* (Hnilica, L. S., Stein, G. S., and Stein, J. L., Eds.) pp 165–182, CRC Press, Boca Raton, FL.
- Wouters-Tyrou, D., Martinage, A., Chevaillier, P., and Sautiere, P. (1998) *Biochimie* 80, 117–128.
- Hecht, N. B. (1998) *BioEssays* 20, 555–561.
- Singh, J., and Rao, M. R. S. (1987) *J. Biol. Chem.* 262, 734–740.
- Baskaran, R., and Rao, M. R. S. (1991) *Biochem. Biophys. Res. Commun.* 179, 1491–1499.
- Baskaran, R., and Rao, M. R. S. (1990) *J. Biol. Chem.* 265, 21039–21047.
- Kundu, T. K., and Rao, M. R. S. (1994) *FEBS Lett.* 351, 6–10.
- Kundu, T. K., and Rao, M. R. S. (1995) *Biochemistry* 34, 5143–5150.
- Kundu, T. K., and Rao, M. R. S. (1996) *Biochemistry* 35, 15626–15632.
- Meetei, A. R., Ullas, K. S., and Rao, M. R. S. (2000) *J. Biol. Chem.* 275, 38500–38507.
- Akama, K., Ichimura, H., Sato, H., Kojima, S., Miura, K., Hayashi, H., Komatsu, Y., and Nakano, M. (1995) *Eur. J. Biochem.* 233, 179–185.
- Hunter, T. (1987) *Cell* 50, 823–829.
- Hunter, T., and Karin, M. (1992) *Cell* 70, 375–387.
- Strahl, B. D., and Allis, C. D. (2000) *Nature* 403, 41–45.
- Sung, M. T., and Dixon, G. H. (1970) *Proc. Natl. Acad. Sci. U.S.A.* 67, 1616–1623.
- Pirhonen, A., Valtonen, P., Linnala-Kankkunen, A., and Maenpaa, P. H. (1993) *Biol. Reprod.* 48, 821–827.
- Pirhonen, A., Linnala-Kankkunen, A., and Menpaa, P. H. (1994) *Eur. J. Biochem.* 223, 165–169.
- Pirhonen, A., Linnala-Kankkunen, A., and Maenpaa, P. H. (1994) *Biol. Reprod.* 50, 981–986.
- Bode, J., Willmitzer, L., and Opatz, K. (1977) *Eur. J. Biochem.* 72, 393–403.
- Marushige, Y., and Marushige, K. (1978) *Biochim. Biophys. Acta* 518, 440–449.
- Green, G. R., Balhorn, R., Poccia, D. L., and Hecht, N. B. (1994) *Mol. Reprod. Dev.* 37, 255–263.
- Oliva, R., and Dixon, G. H. (1991) *Prog. Nucl. Res. Mol. Biol.* 40, 25–94.
- Levesque, D., Veilleux, S., Caron, N., and Boissonneault, G. (1998) *Biochem. Biophys. Res. Commun.* 252, 602–609.
- Platz, R. D., Meistrich, M. L., and Grimes, S. R. (1977) *Methods Cell Biol.* 16, 297–316.
- Meetei, A. R., and Rao, M. R. S. (1996) *Protein Expression Purif.* 8, 409–415.
- Meetei, A. R., and Rao, M. R. S. (1998) *Protein Expression Purif.* 13, 184–190.
- Meetei, A. R., and Rao, M. R. S. (1998) *Anal. Biochem.* 264, 288–291.
- Laemmli, U. K. (1970) *Nature* 227, 680–685.
- Panyim, S., and Chalkley, R. (1969) *Arch. Biochem. Biophys.* 130, 337–346.
- Wang, M. S., Pang, J. S., and Selsted, M. E. (1997) *Anal. Biochem.* 253, 225–230.
- Kamps, M. P., and Sefton, B. M. (1989) *Anal. Biochem.* 176, 22–27.
- Boyle, W. J., van der Geer, P., and Hunter, T. (1991) *Methods Enzymol.* 201, 110–149.
- Kundu, T. K., Meetei, A. R., and Srinath, B. R. (1995) *J. Biochem. Biophys. Methods* 30, 185–189.
- Baskaran, R., and Rao, M. R. S. (1990) *J. Biol. Chem.* 265 (34), 21039–21047.
- Colledge, M., and Scott, J. D. (1999) *Trends Cell Biol.* 9, 216–221.
- Edwards, A. S., and Scott, J. D. (2000) *Curr. Opin. Cell Biol.* 12, 217–221.
- Mei, X., Singh, I. S., Erlichman, J., and Orr, G. A. (1997) *Eur. J. Biochem.* 246, 425–432.
- Johnson, L. R., Foster, J. A., Haig-Ladeorg, L., Vanscoy, H., Rubin, C. S., Moss, S. B., and Gerton, G. L. (1997) *Dev. Biol.* 192, 340–350.
- Visconti, P. E., Johnson, L. R., Oyaski, M., Fornes, M., Moss, S. B., Gerton, G. L., and Kopf, G. S. (1997) *Dev. Biol.* 192, 351–363.
- Vijayaraghavan, S., Liberty, G. A., Mohan, J., Winfrey, V. P., Olson, G. E., and Carr, D. W. (1999) *Mol. Endocrinol.* 13, 705–717.
- Collas, P., Le Guellec, K., and Tasken, K. (1999) *J. Cell Biol.* 147, 1167–1180.
- Kundu, T. K., and Rao, M. R. S. (1999) *J. Biochem.* 125, 217–222.
- Rauskas, E., and Mikelsaar, R. H. (1999) *BioEssays* 21, 440–448.
- Wu, J. Y., Ribar, T. J., Cummings, D. E., Burton, K. A., McKnight, G. S., and Means, A. R. (2000) *Nat. Genet.*, 25, 448–452.
- Gatewood, J. M., Cook, G. R., Balhorn, R., Bradbury, E. M., and Schmid, C. W. (1987) *Science* 236, 962–964.
- Pittoggi, C., Renzi, L., Zaccagnini, G., Cimini, D., Degraffi, F., Giordano, R., Magnano, A. R., Lorenzini, R., Lavia, P., and Spadafora, C. (1999) *J. Cell Sci.* 112, 3537–3548.

BI0117652